

THE CREATION OF THE RARE LIGHT ELEMENTS -
IMPLICATIONS FOR COSMOLOGY

SAM M. AUSTIN
Cyclotron Laboratory and Physics Department,
Michigan State University, East Lansing, Michigan 48824,
U.S.A.

Abstract

THE CREATION OF THE RARE LIGHT ELEMENTS - IMPLICATIONS FOR COSMOLOGY.

1. Introduction; 2. Creation of the Rare Light Elements in the Galactic Cosmic Rays; 2.1. General Theory; 2.2. Techniques for Measuring Spallation Cross Sections; 2.3. Time of Flight Measurements; 2.4. Calculations of RLE Production in the Galactic Cosmic Rays - Comparison with Experimental Abundances; 3. Creation of the Rare Light Elements in a Big Bang; 3.1. Basic Cosmology; 3.2. Results of Standard Big Bang Calculations; 4. Cosmological Implications; 4.1. Constraints on the Mean Baryon Density P_b from the Deuterium Abundance; 4.2. Constraints on P_b from the Abundance of ${}^7\text{Li}$; 5. Summary and Conclusions.

1. INTRODUCTION

It appears that most elements with mass $A \geq 12$ are synthesized in the centers of stars during their static burning stages and the supernovae that end their lives [1,2]. Most of the lighter elements, on the other hand, are too fragile to survive the temperatures and densities found in stellar centers and must therefore be created in a cooler and/or less dense environment. As a result, with the single exception of ${}^4\text{He}$, these light elements are found in nature with abundances much less than those of their neighbors (see Fig. 1) and are collectively known as the rare light elements (RLE).

In recent years there has been great progress in understanding the processes which create the RLE. An unexpected byproduct of this understanding is the most convincing answer to date of the cosmological question: will the presently observed expansion of the Universe continue forever, or will the Universe eventually collapse again to a hot dense singularity? This talk will review theories of

the creation processes for the RLE, with emphasis on the role played by nuclear physics. In particular, techniques for the measurement of spallation cross sections which play an important role in various theories will be discussed in some detail. Finally I will review the implications of RLE production for cosmology and will show that the abundances of ${}^2\text{H}$ and ${}^7\text{Li}$ can be used to place limits on the mean baryon density of the Universe. In the simplest model, these limits imply that the expansion of the Universe will continue forever.

2. CREATION OF THE RARE LIGHT ELEMENTS IN THE GALACTIC COSMIC RAYS.

The requirement that the rare light elements are formed in a relatively cool tenuous medium is such a strong constraint that until recently there were no viable candidates for creation sites. Formation by spallation in particle flares at stellar surfaces appeared promising but was later found to be energetically difficult [4], requiring that essentially all available gravitational energy be converted to the kinetic energy of the flare particles. A clue, which, with hindsight, points inevitably to an important creation mechanism is contained in Fig. 1. Namely, that the abundances of the elements Li , Be and B are much greater in the cosmic rays than in the solar system. (The same is true for elements just below the iron peak.) It is possible to understand these differences by postulating that during their flight to the neighborhood of the earth, the more abundant elements C , N , O interacted with particles in the interstellar medium to form the RLE; such theories are able to reproduce the observed cosmic ray spectra in some detail. Since some of the Li , Be , B so created will thermalize and become part of the interstellar medium, eventually to be incorporated into stars, the process clearly contributes to the observed abundance of these elements. One must

however ascertain whether the creation process is quantitatively effective. Reeves, Fowler and Hoyle [5] were first to consider this process in detail.

2.1. General Theory

In the simplest possible calculation, ignoring variations in time of the cosmic ray flux, processing of the produced RLE matter in stars, etc. [6], the yield per unit time of an element *i* is given by

$$Y_i = \int_{p,t} N_t \int_0^\infty \phi_p(E) \sigma_{pt}^i(E) dE$$

where $\phi_p(E)$ is the flux of the cosmic ray projectile *p*, N_t is the number density of the interstellar target *t* and $\sigma_{pt}^i(E)$ is the cross section for formation of nuclide *i* in a collision of *p* and *t*. The summation is over all possible projectiles and targets. One obtains the cosmic ray flux from available measurements after a difficult and uncertain correction for the effects of modulation by electromagnetic fields encountered near the earth. The target density is taken from solar system abundances [7] and one needs only the relevant spallation cross sections to evaluate the production of a given nuclide.

The most important reactions involve those for which the product $N_t \phi_p$ is large. Table I shows a typical set of such values, normalized to $N_t \phi_p = 1.0$.

TABLE I. ENUMERATION OF ASTROPHYSICALLY IMPORTANT SPALLATION PROJECTILES AND TARGETS

Nuclide (p or t)	N_t (a)	ϕ_p (b) ($E_p > 2$ GeV)
p	1.0	1.0
⁴ He	0.069	0.059
¹² C	3.7×10^{-4}	1.7×10^{-3}
¹⁴ N	1.1×10^{-4}	4.7×10^{-4}
¹⁶ O	6.7×10^{-4}	1.5×10^{-3}

(a) Ref. [7] normalized to $N_t = 1.0$ for protons
 (b) Ref. [6] normalized to $\phi_p = 1.0$ for protons

ized to hydrogen. One sees immediately that the reactions $p + CNO$ will be important for production of all the RLE, with the $\alpha\alpha$ reactions contributing to the production of ⁶Li and the p^4He reactions to ²H, ³H, ³He. The $\alpha + CNO$ reactions are not entirely negligible [8], adding perhaps 10-20% to the yield of the RLE from the $p + CNO$ reactions.

2.2. Techniques for Measuring Spallation Cross Sections.

Because one needs the yields for stable as well as radioactive nuclei, the measurement of radioactivity following bombardment of a target, while simple, is sufficient or useful only in a few special cases (e.g. production of ¹⁰Be for use as a clock for cosmic ray age [6], or ⁷Be for use as an absolute standard in the mass-spectrographic measurements described in section 2.2.2). Straightforward measurements of the double differential cross section $\frac{d^2\sigma}{dE d\Omega}$ using standard $\Delta E-E$ telescopes for particle identification are also not generally applicable. The bulk of the yield often lies at such low energies that either the particle does not penetrate the ΔE telescope or the $\Delta E, E$ information is insufficient to identify the particle uniquely. We describe briefly below several techniques which have been applied to this problem.

2.2.1. Nuclear Emulsions.

A number of experiments [9] have employed nuclear emulsions as targets. But because of difficulties identifying the target species and because reactions yielding neutral particles may go undetected, the results obtained have often been in disagreement with better established procedures.

2.2.2. Mass Spectroscopy.

The target material is bombarded by an intense flux of high energy protons or alpha particles. The small quantity (10^{-9} - 10^{-12} g) of a product nuclide is separated from the target and the relative yields of products are measured in a sputtering mass spectrometer [10]. Isotope dilution procedures or known radioactive cross sections are then used to determine the absolute yields. This procedure has been carried out successfully at Orsay (see [8] and references therein) and yielded the first reliable measurements of cross sections for the stable elements. It is applicable at all energies and in principle to all targets, but is extremely tedious and difficult. For example, one needs to develop a new procedure for each target-projectile combination. Nevertheless, most available cross sections at energies above 100 MeV have been measured in this way.

2.2.3. Relativistic Heavy Ions.

In the converse of the usual procedure one accelerates heavy ions such as C, N or O to high energies and allows them to strike targets of H or He. The RLE produced emerge with rather small transverse momenta and almost the same velocity as the beam. They are therefore tightly collimated in the forward direction and are relatively simple to detect and identify. This technique is of great generality, being applicable to any target-projectile combination once the heavy ion beam is developed [11]. Its major limitation appears to be a restricted energy range, the lower energy limit being set by the finite transverse momenta which eventually make separation of adjoining isotopes difficult, and the upper energy limit by the available energy of heavy ion beams (≤ 2.1 GeV per nucleon).

2.2.4. Time of Flight.

A pulsed beam of protons or alpha particles strikes a target, and the RLE produced are detected in a detector which measures both their energy E and time of flight from the target, T. One then calculates the product $E T^2$ which is proportional to the product mass. Because only a single detector is involved, the low energy cut-off can be 0.5 MeV or less, thus including the great bulk of the RLE energy spectrum. Having measured the double differential cross section, $\frac{d^2\sigma}{dE d\Omega}$, the total yield is obtained by integration. This technique is applicable in principle to all projectiles and targets and has been used extensively at bombarding energies of 100 MeV and below. An apparent limitation is that only the mass of the product particle can be determined. But since in most cases only a single isotope of a given mass is stable on astrophysical time scales (for example ^{11}C decays to ^{11}B with $\tau_{1/2} = 20$ min and hence for most astrophysical purposes is equivalent to ^{11}B) this is not often a limitation. Exceptions are ^{10}Be with $\tau_{1/2} = 1.5 \times 10^6$ years, and ^9C which β decays to ^9B which is particle unstable.

2.3. Time of Flight (TOF) Measurements

Because a pulsed beam is required for TOF measurements, they are particularly well suited to cyclotrons where the beam is naturally pulsed at a convenient repetition rate. These measurements were first carried out at Michigan State University [12] and more recently at the Universities of Washington [13] and Maryland [14]. I will discuss here the work at MSU, primarily for reasons of familiarity; a summary of this and other work using the TOF techniques is shown in Table II. Work by other techniques has been summarized recently in refs. [8, 11, 15].

TABLE II. SPALLATION CROSS SECTION MEASUREMENTS USING THE TIME-OF-FLIGHT TECHNIQUE

Reaction	Energies (MeV)	Reference
p+ ¹² C	22-44 45-100	16 14
p+ ¹³ C	5-18	17
p+ ¹⁴ N	17-42 75,90	18 19
α+ ¹⁴ N	21-42	13
p+ ¹⁶ O	30-42 50-90	20 19
p+ ²⁰ Ne	30-40	21

Stringent phase selection applied near the center of the MSU cyclotron typically limits the burst width to less than 400 psec (see Fig. 2) permitting adequate particle identification with a 25-30 cm flight path. For such a short flight path it is unnecessary to remove beam bursts to obtain an adequate dynamic range in energy. Thus count rates are strongly related to the time resolution. (At higher energies where a greater dynamic range may be required, or when intrinsic time resolution of the accelerator is poorer, it may be advantageous to obtain the zero (start signal) for the time of flight from a carbon-foil-chevron-plate detector placed near the target [19]). Particles were detected in a thin overbiased silicon counter. A solid target was used for ¹²C and gaseous targets for ¹⁴N, ¹⁶O and ²⁰Ne. Special gas cell techniques [22] were required because of the low energy of the RLE products and the stringent requirement on the effective length of the irradiated area necessary to preserve good time resolution. The mass resolution obtained is shown for a ¹²C target in Fig. 3; it is clearly sufficient to separate the RLE reaction products of interest. A typical spallation spectrum for masses 6 and 7 is in Fig. 4. While two-body channels are important, the bulk of the

yield is contained in a multiparticle continuum extending to the lowest observed energies. At still lower energies the spectrum must turn over and approach zero as E→0 [16]. Figs. 5 and 6 show the experimental results for the most thoroughly studied case to date, ¹²C + p. The MSU and Maryland TOF results (Fig. 5) are in very good agreement with each other and with isolated mass spectroscopic results (not shown). There are strong threshold effects but the cross sections appear to approach constant values at the higher energies. For most of the isotopes, it is in fact a reasonable approximation to assume that the cross sections are constant beyond 100 MeV. The accuracy of this assumption is indicated in Fig. 6 where available ¹²C+p cross sections are shown for energies between 100 and 10,000 MeV. Data at 300 GeV [8] strengthen this conclusion. The α+p reactions also contribute significantly to the production of masses 6 and 7. Cross sections measured recently at MSU [23,24], Maryland [24] and Orsay [25] are shown in Fig. 7. Experimental spallation cross sections are now available for nearly all important reactions and the theoretical calculations of RLE production are on a much firmer basis than before.

Only a few measurements of cross sections are available for production of RLE when the important astrophysical targets ¹²C, ¹⁴N, ¹⁶O are bombarded by α particles. Such measurements could be carried out at the B.A.R.C. Cyclotron and would be particularly important in evaluating the effects of alternate mechanisms for production of the RLE mentioned in section 2.4.

2.4. Calculations of RLE Production in the Galactic Cosmic Rays - Comparison with Experimental Abundances

In this section, we will discuss mainly the results of Meneuzzi

TABLE III. ABUNDANCES AND PRODUCTION IN THE GALACTIC COSMIC RAYS OF THE RARE LIGHT ELEMENTS

Nuclide	(a) Abundance	Ref	GCR PRODUCTION (a)				Agreement of Experi- ment and Theory
			(b) Meneguzzi[6]	(c) Reeves[30]	(d) Mitler[26]	(e) Miller[26]	
^2H	$(1.8 \pm 0.4) \times 10^{-5}$	28, 29				10^{-8}	Poor
^3He	2×10^{-5}	15				10^{-8}	Poor
^6Li	7.6×10^{-11}	27	8.2×10^{-11}	5×10^{-11}		9×10^{-11}	Good
^7Li	92×10^{-11}	27	12×10^{-11}			$14 \times 10^{-11(e)}$	Poor
^9Be	1.3×10^{-11}	27	2.0×10^{-11}	1.3×10^{-11}		1.7×10^{-11}	Good
^{10}B	2×10^{-11}	27	8.6×10^{-11}	5×10^{-11}		5.2×10^{-11}	OK
^{11}B	8×10^{-11}	27	21×10^{-11}	12×10^{-11}		14×10^{-11}	OK

(a) Number ratio relative to ^1H i.e.: $N(i)/N(^1\text{H})$

(b) From Table 5, Column 2 of Ref [6].

(c) Results of Ref. [6] adjusted [30] to fit ^9Be abundance

(d) From Table 5, Column 9 of Ref [26]

(e) Corrected for new measurement of $\alpha + \alpha$ (mass 7) cross section [23, 24]

et al. [6]. In these calculations, the cosmic-ray transport problem is treated carefully, but certain simplifying assumptions are made: namely that the cosmic-ray flux is independent of time and that the net effects of astration (stellar processing) are negligible. Calculations of Mitler [26] including these effects show that they tend to cancel, and yield results quite close to those of Meneguzzi et al. All of these calculations were made using estimated $\alpha + \alpha$ mass 7 cross sections which are larger than the recent measurements. Thus they overestimate the production of ^7Li .

The predicted yields for ^6Li and ^7Li are shown as a function of time in Fig. 8. Two values of the observed abundance are shown for each nucleus. One of these is the meteoritic abundance, and is presumably equal to the interstellar abundance when the solar system was formed approximately 4.6×10^9 years ago, while the other is the observed abundance in newly formed stars and is presumably equal to the present interstellar abundance. (In the case of ^6Li only an upper limit is available for the stellar abundance.) These and the other abundances shown in Table III are mostly from the survey by Boesgaard [27].

One finds that spallation in the galactic cosmic rays can explain the observed abundance of ^6Li , but fails in the case of ^7Li by a factor of about 7 or 8. Comparisons similar to the above for the other RLE lead to the results shown in Table III. Spallation of the galactic cosmic rays produces very little ^2H , ^3He and ^4He ; about 15% of the observed ^7Li and within uncertainties approximately all of the isotopes ^6Li , ^9Be , ^{10}B and ^{11}B . Discrepancies of roughly a factor of 2 remain in some cases but are probably within the uncertainties involved in these calculations and in the abundance measurements.

A nagging difficulty is that it is difficult to reproduce the well known value for the ratio of ^{11}B to ^{10}B : $^{11}\text{B}/^{10}\text{B} = 4.1$, most calculations yielding values between 2 and 3. It is not clear whether this is a fundamental problem rooted in the basic theory of the process or a measure of the remaining approximations in the calculations. The abundance of $^{11}\text{B} + ^{10}\text{B}$ is also rather uncertain -- see Refs. [15, 27] for a detailed discussion. In summary, while one can produce some of the RLE in their observed abundances, it remains to find the sources of ^2H , ^3He , ^4He and ^7Li .

One possibility is that at least some of the RLE are produced by fluxes of projectiles with energies in the range of tens of MeV per nucleon. For these energies the reactions with low thresholds, namely: $p + ^{13}\text{C}$, $p + ^{14}\text{N}$ and $\alpha + \alpha$ dominate the yield of RLE. Bodansky, Jacobs and Oberg [31] concluded that a suitably chosen flux of protons and α particles, with selected energies less than 25 MeV per nucleon, could reproduce many of the features of the observed abundances.

although somewhat ad hoc assumptions were required to obtain the presently accepted B abundance. However, it is not clear that a source of such energetic particles exists in nature in combination with the required low temperature and/or density. It has been suggested that a suitable site is shock waves in supernovae. However it now appears that it is difficult to obtain projectiles of sufficient energy and that even if one could, conditions yielding sufficient ${}^2\text{H}$ would usually overproduce the other light elements. Eprtain, Arnett and Schramm [32] discuss this mechanism in detail. Another possibility is spallation in a low-energy component of the cosmic rays so far unobserved because of shielding by the solar wind in the neighborhood of the earth. There is at present no direct evidence for such particles and constraints on their abundance and spectra from the observed ionization [6] of interstellar hydrogen may make this hypothesis untenable. Stellar flares analogous to those on the sun are another possibility. Solar flares are observed to contain particles with energies up to about 50 MeV per nucleon. Again the major difficulty is that one can obtain a sufficient particle flux only by somehow converting an unlikely fraction of all available energy into flare-particle energy. These and several other possibilities and their attendant difficulties are discussed in Reeves [15].

We consider next the most promising possibility: production of the RLE in a primordial big bang.

3. CREATION OF THE RARE LIGHT ELEMENTS IN A BIG BANG.

3.1. Basic Cosmology.

A number of excellent reviews [29,33] of the big bang model and of nucleosynthesis in a big bang have been published recently. We

review here only those aspects which are particularly pertinent to the creation of the rare light elements. The basic picture is that the universe was once small and at a temperature sufficiently high to impose statistical equilibrium among all particles present ($T \approx 10^{11}$ K). Expansion from this initial state is continuing today, as is qualitatively evidenced by the observed recession of all distant galaxies. The most convincing evidence for the Big Bang is the record of the initial hot dense state found in the background microwave radiation, which is nearly isotropic and has a black body spectrum characterized by $T = 2.90 \pm 0.08^\circ\text{K}$.

One must determine the nature of this universe from experiments. If it is assumed that the cosmological constant Λ is 0, then the nature of the possible solutions depends only on the mean baryon density ρ_b of the universe. It is useful to define a critical density ρ_c

$$\rho_c = \frac{3H_0^2}{8\pi G} = 5.7 \times 10^{-30} \left(\frac{H_0}{55}\right)^2 \text{ g/cm}^3$$

where H_0 , the Hubble constant (in units of $\text{km sec}^{-1} \text{Mpc}^{-1}$) relates the observed recessional velocity v of a distant galaxy to its distance r according to $v = H_0 r$. Then the solutions can be classified by the value of the ratio ρ_b/ρ_c as is shown in Fig. 9. In the low density case ($\rho_b/\rho_c < 1$) the universe is open, has the escape velocity and will continue to expand forever, while in the high density case ($\rho_b/\rho_c > 1$) the universe is closed and will eventually collapse again to a hot dense singularity. Since $H_0 \approx 55 \text{ km sec}^{-1} \text{Mpc}^{-1}$, $\rho_c \approx 5.7 \times 10^{-30} \text{ gm/cm}^3$.

3.2. Results of Standard Big-Bang Calculations.

If one imposes, in addition to those mentioned earlier, the

further assumptions that,

- 1) general relativity is the correct theory of gravity;
- 2) the Universe is homogeneous and isotropic;
- 3) only presently known particles were present during nucleosynthesis;
- 4) the baryon number of the Universe is positive; and
- 5) all types of neutrinos are nondegenerate;

then one obtains the so-called "standard" big-bang model [29] for which most calculations have been made. Besides a gravitational theory, one needs the rates for a rather large number of reactions as shown in the reaction network of Fig. 10. These rates are relatively well known with one exception, that which dominates the synthesis of ${}^6\text{Li}$ [29] and permit calculation of nucleosynthesis yields to better than a factor of two [34], again excepting ${}^6\text{Li}$. Detailed calculations of the standard big bang have been carried out by Wagoner [34] and show that nucleosynthesis takes place 100-1000 sec after the beginning of the expansion when the temperature is near 10^9 °K, and density near 1 mg/cm^3 . The mass fraction X_i of a given isotope i produced during the Big Bang depends only upon ρ_b as is shown in Fig. 11. Only ${}^2\text{H}$, ${}^3\text{He}$ and ${}^7\text{Li}$, precisely those elements not made in the galactic cosmic rays, are made in significant quantities.

The predicted helium abundance is particularly useful for verifying the assumptions of the standard big bang model. There is strong evidence [29] that ${}^4\text{He}$ is made in a big bang. If one substantially relaxes any of the standard big bang assumptions the ${}^4\text{He}$ abundance is not reproduced [29], lending confidence that the apparently extreme assumptions of the standard big bang are approximately correct. Once one accepts these calculations, the abundances of ${}^2\text{H}$ and ${}^7\text{Li}$ place extremely strong constraints on the nature of the Universe.

4. COSMOLOGICAL IMPLICATIONS.

The basic principle invoked is that the abundance of an element produced in a big bang depends on the density. This dependence is especially strong in the case of ${}^2\text{H}$ and ${}^7\text{Li}$. Consequently if one believes that an element is made only in a big-bang explosion, its observed abundance immediately fixes the mean baryon density of the Universe.

4.1. Constraints on ρ_b from the Deuterium Abundance.

It has been pointed out by Wagoner [34] and others, and most forcefully by Gott et al. [35], that the observed abundance of ${}^2\text{H}$ can be used to estimate the mean baryon density ρ_b of the Universe. This estimate rests on the facts that there is no plausible source of ${}^2\text{H}$ other than the primordial Big Bang, and that the production of ${}^2\text{H}$ in the standard big bang decreases rapidly with increasing ρ_b . If one then assumes that all ${}^2\text{H}$ was formed in a big bang and corrects the abundance by about a factor of 2 to account for the amount destroyed by astration, one obtains $\rho_b = 4 \times 10^{-31} \text{ g/cm}^3$. This is roughly an order of magnitude less than the critical density, leading to the conclusion [35] that the Universe is open and will continue to expand forever.

A major weakness in this argument is that one may find another source of ${}^2\text{H}$. For example, it has been suggested that ${}^2\text{H}$ could be made in shock waves accompanying a supernova explosion. This particular mechanism now seems unlikely [32], but the fertile minds at work on the problem will certainly suggest other possible sources, so it is important to obtain confirming evidence for the above conclusion. We now show that the observed abundance of ${}^7\text{Li}$ can provide just such evidence.

4.2. A Constraint on ρ_b from the Abundance of ${}^7\text{Li}$.

The major difficulty in using ${}^7\text{Li}$ to obtain an estimate of the universal density is that there are many possible sources of ${}^7\text{Li}$ (some of which have been discussed briefly in an earlier section). Fortunately, however, the mass fraction X_7 of ${}^7\text{Li}$ produced increases with increasing density in the relevant density region. Consequently, ${}^7\text{Li}$ can be used [36] to place an upper limit on ρ_b , even if other production mechanisms are important by assuming that all the ${}^7\text{Li}$ is made in the Big Bang. This upper limit is $\rho_b \leq 1.1 \times 10^{-30} \text{ g/cm}^3$. Again $\rho_b < \rho_c$ implying that the Universe is open.

The major uncertainty in the case of ${}^7\text{Li}$ contrasts nicely with that for ${}^2\text{H}$. For ${}^7\text{Li}$, discovery of other sources of ${}^7\text{Li}$ leads to a stronger upper limit. But if a substantial fraction of interstellar material is astrated, and the lithium thereby destroyed, the Big Bang could have made a larger amount of ${}^7\text{Li}$, weakening the upper limit.

Further complicating the picture is the possibility that infall of primordial material from the galactic halo may be significant [15] and could tend to compensate the efforts of astration for those nuclei produced in the Big Bang.

If it is a good approximation to ignore both astration and sources of ${}^2\text{H}$ and ${}^7\text{Li}$ other than the big bang, then their observed abundances each separately determine the density. When the possible contributions to ${}^7\text{Li}$ by other sources is better understood, the requirement that the big bang contributions to the abundances X_D and X_7 yield the same value of ρ_b may yield strong constraint on allowable astration, and hence, on models of galaxy formation. Fig. 12 shows the values of ρ_b determined from ${}^2\text{H}$ and ${}^7\text{Li}$ (neglecting both astration and other sources) and the abundances on which they were based.

These ρ_b are in excellent agreement. Substantial astration of ${}^2\text{H}$ and ${}^7\text{Li}$ would tend to worsen the agreement while discovery of other sources of ${}^7\text{Li}$ could improve it slightly. Also shown on Fig. 12 is an estimate of the density of material in galaxies [35,33] evaluated at $H_0 = 55 \text{ sec km}^{-1} \text{ Mpc}^{-1}$. Combining this lower limit on ρ_b with the upper limit based on the abundances constrains the density to lie in a rather narrow band: $3 \times 10^{-31} \leq \rho_b \leq 1 \times 10^{-30} \text{ g/cm}^3$.

While the presentation of Fig. 12 is most direct, it is also instructive to plot the constraints on a graph with ρ/ρ_c as the abscissa and H_0 as the ordinate. This presentation allows one to conveniently apply the weaker constraints from astronomical data (e.g. the age of the Universe and the so-called deceleration parameter). One can show that H_0 is constrained to $495H_0 \leq 65 \text{ km sec}^{-1} \text{ Mpc}^{-1}$ with density constraints consistent with those of Fig. 12.

5. SUMMARY AND CONCLUSIONS.

5.1. Abundances of the RIE.

The simplest picture consistent with the available data is that ${}^6\text{Li}$, ${}^9\text{Be}$, ${}^{10}\text{B}$, ${}^{11}\text{B}$ are made in the galactic cosmic rays, while ${}^2\text{H}$, ${}^3\text{He}$, ${}^4\text{He}$ and ${}^7\text{Li}$ are made in the primordial big bang. While the uncertainties in the abundances and in the theory clearly permit other interpretations, they are certainly not required at this stage.

5.2. Implications for Cosmology.

If the Universe is a Friedmann Universe, with cosmological constant $\Lambda=0$, it is open and the present expansion will continue forever. This conclusion does however rest on the assumption that $\Lambda=0$. While this value is consistent with the available data, a non-zero value cannot be excluded, except on aesthetic grounds, and its effects must

be considered [33]. It has been found [33] that for reasonable values of A the limits on ρ_b from the ^2H and ^7Li abundances are essentially unchanged. However, the simple connection of ρ_b to the curvature and future evolution of the Universe is no longer valid. One requires additional information to fix these properties. Tinsley [33] has discussed this problem in some detail and concludes that the most likely such evidence would be the direct measurement of the lifetime of the Universe.

ACKNOWLEDGEMENTS

I gratefully acknowledge the dominant contributions to the experimental work reported here of my collaborators: W.S. Chien, C.N. Davids, H. Laumer, C.H. King, L.M. Panggabean and H. Rossner from MSU and G. Mathews and V. Viola from the University of Maryland. I wish to thank D.N. Schramm and R. Stein for valuable discussions.

This research was supported by the U.S. National Science Foundation.

REFERENCES

1. CLAYTON, D.D., Principles of Stellar Evolution and Nucleosynthesis; McGraw Hill, New York (1968).
2. SCHRAMM, D.N., ARNETT, W.D., Explosive Nucleosynthesis; U. of Texas Press, Austin (1973).
3. MEYER, P., RAMATY, R., WEBER, W.R., Phys. Today 27 No.10(1974)23.
4. RYTER, C., REEVES, H., GRADSTAJN, E., Astron. Ap. 8 (1970) 389.
5. REEVES, H., FOWLER, W.A.; HOYLE, F., Nature 226 (1970) 727.
6. NENEKUZZI, N., AUDOUZE, J., REEVES, H., Astron. Ap. 15 (1971) 837.
7. CAMERON, A.G.W., Sp. Sci. Rev. 15 (1973) 121.

8. RATSBECK, G.M., YIOU, F., In Spallation Reactions and Their Applications; P. Reidel (1976).
9. JUNG, M., JACQUOT, C., BAIXERAS-AIGUABELLA, C., SCHMITT, R., BRAUN, H., Phys. Rev. C1 (1970) 435; JUNG, M., JACQUOT, C., BAIXERAS-AIGUABELLA, C., SCHMITT, R., BRAUN, H., GIRARDIN, L., Phys. Rev. 188 (1969) 1517.
10. FONTES, P., PERRON, C., LESTRINGUEZ, J., YIOU, F., BERNAS, R., Nucl. Phys. A165 (1971) 405.
11. HECKMAN, H.H., GREINER, D.E., LINDSTROM, P.J., BIESER, F.S., Phys. Rev. Lett. 28 (1972) 926; GREINER, D.E., LINDSTROM, P.J., HECKMAN, H.H., CORK, B., BIESER, F.S., Phys. Rev. Lett. 35 (1975) 152; LINDSTROM, P.J., GREINER, D.E., HECKMAN, H.H., CORK, B., BIESER, F.S., Lawrence Berkeley Laboratory Report LBL-4650, unpublished (1975).
12. DAVIDS, C.N., LAUMER, H., AUSTIN, S.M., Phys. Rev. Lett. 22 (1969) 1388.
13. JACOBS, W.W., BODANSKY, D., CHAMBERLIN, D., OBERG, D.L., Phys. Rev. C9 (1974) 2134.
14. ROCHE, C.T., CLARK, R.G., MATHEWS, G.J., VIOLA, V.E., Phys. Rev. C14 (1976) 410.
15. REEVES, H., Ann Rev. Astron. Ap. 12 (1974) 437.
16. DAVIDS, C.N., LAUMER, H., AUSTIN, S.M., Phys. Rev. C1 (1970) 270.
17. OBERG, D.L., BODANSKY, D., CHAMBERLIN, D., JACOBS, W.W., Phys. Rev. C11 (1975) 410.
18. LAUMER, H., AUSTIN, S.M., PANGGABEAN, L.M., DAVIDS, C.N., Phys. Rev. C8 (1973) 483.
19. HOYLE, R.A., GLAGOLA, B.G., MATHEWS, G.J., VIOLA, V.E., Bull. Am. Phys. Soc. 22 (1977) 998.
20. LAUMER, H., AUSTIN, S.M., PANGGABEAN, L.M., Phys. Rev. C10 (1974) 1045.
21. PANGGABEAN, L.M., AUSTIN, S.M., LAUMER, H., Phys. Rev. C10 (1974) 1605.
22. LAUMER, H., DAVIDS, C.N., AUSTIN, S.M., PANGGABEAN, L.M., Nucl. Instr. Meth. 120 (1974) 535.
23. KING, C.H., AUSTIN, S.M., ROSSNER, H.H., CHIEN, W.S., Phys. Rev. C (to be published).

24. KING, C.H., ROSSNER, H.H., AUSTIN, S.M., CHIEN, W.S., MATHEWS, G.J., VIOLA, JR., V.E., CLARK, R.G., Phys. Rev. Lett. 35 (1975) 988.
25. YIOU, F., RAISEBECK, G.M., QUECHON, H., 15th International Cosmic Ray Conference (1977).
26. MITLER, H., Ap. Sp. Sci. 17 (1972) 186.
27. BOESGAARD, A.M., Pub. Astron. Soc. Pac. 88 (1976) 353.
28. YORK, D.G., ROGERSON, J.B., Ap. J. 203 (1976) 378.
29. SCHRAMM, D.N., WAGONER, R.V., Ann. Rev. Nuc. Sci. 27, to be published.
30. REEVES, H., as quoted in BOESGAARD (Ref. 27).
31. BODANSKY, D., JACOBS, W.W., OBERG, D.L., Astrophys. J. 202 (1975) 222.
32. EPSTEIN, R.; ARNETT, W.D., SCHRAMM, D.N., Ap. J. Suppl. 31 (1976) 111.
33. TINSLEY, B.M., Physics Today 30 No. 6 (1977) 32.
34. WAGONER, R.V., Ap. J. 179 (1973) 343.
35. GOTT, J.R., GUNN, J.E., SCHRAMM, D.N., TINSLEY, B.M., Ap. J. 194 (1974) 543.
36. AUSTIN, S.M., KING, C.H., Nature, to be published.

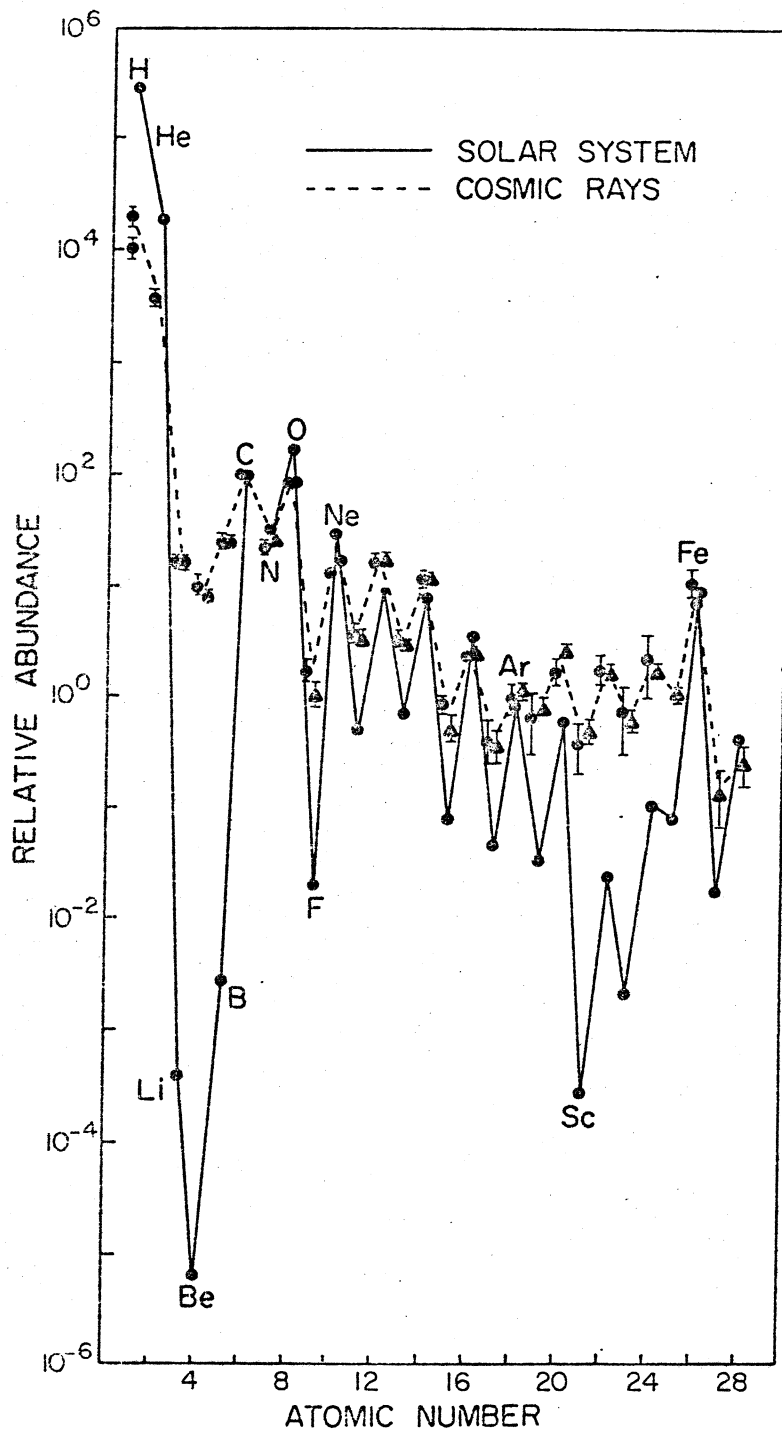


Fig. 1. Relative abundance of the elements ($Z \leq 28$) in the solar system and in the cosmic rays. Abundances are normalized to that of carbon ($C=100$). Adapted from Ref.[3].

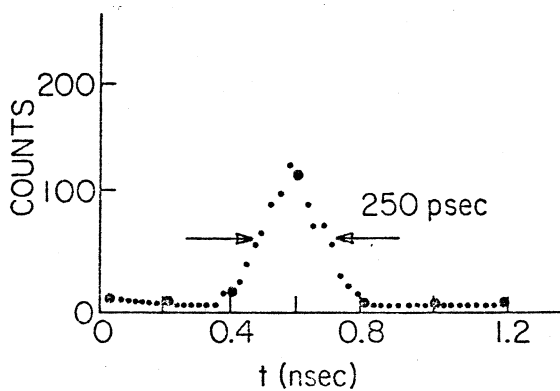


Fig. 2. Time structure of the beam from the MSU cyclotron. The phase selection leading to this burst width is accomplished by slits placed at the 18th and 28th turns of the internal cyclotron beam.

Fig. 4. Energy spectra of masses 6 and 7 following the bombardment of ^{12}C by 39.8-MeV protons. The detector angle is 15° . From Ref. [16].

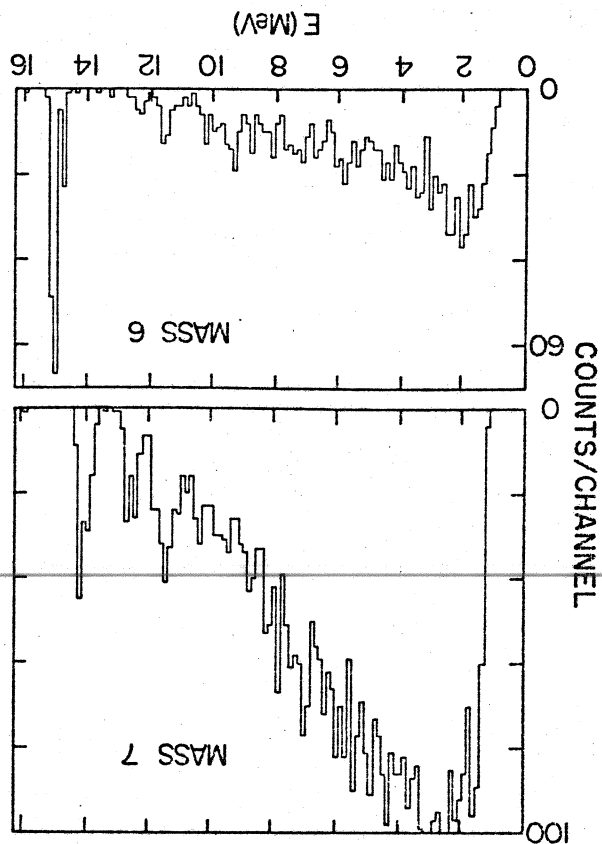
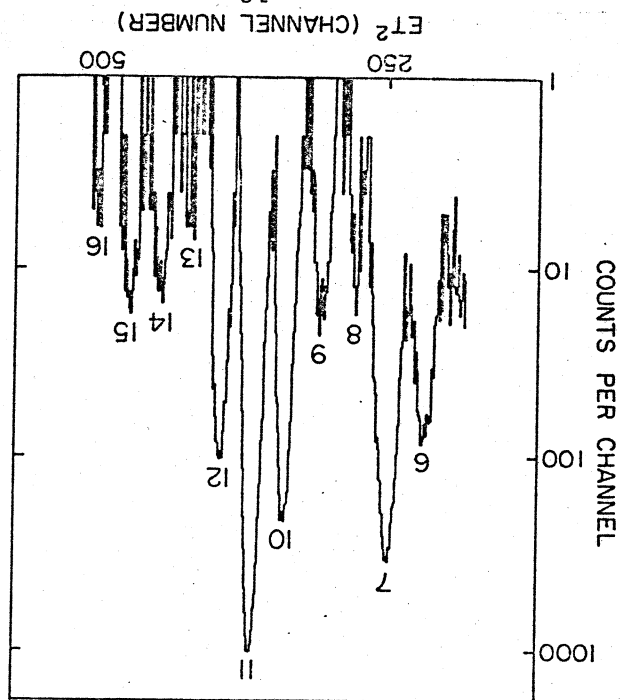


Fig. 3. Mass spectrum from the $^{12}\text{C} + p$ reaction at 40 MeV. The target contains a small ^{16}O impurity.



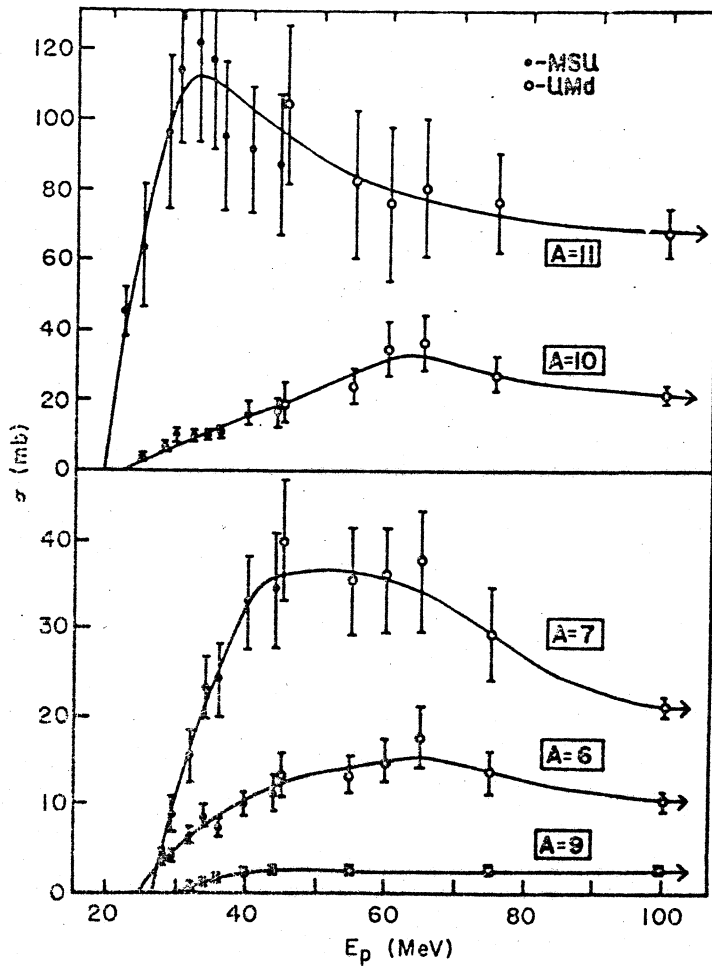


Fig. 5. Spallation cross sections for the $^{12}\text{C}+p$ reaction. Results for $E_p \leq 45$ MeV are from Ref. [16] and those for $E_p > 45$ MeV from Ref. [14]. Fig. from Ref. [14].

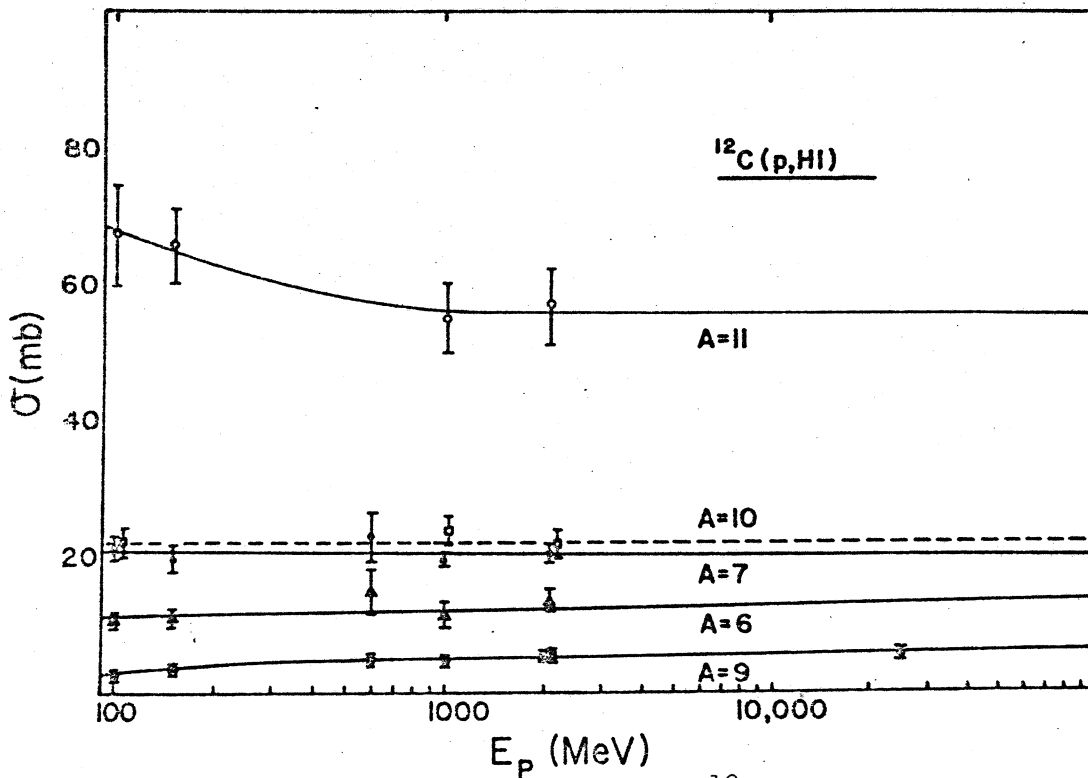


Fig. 6. Spallation cross sections for the $^{12}\text{C}+p$ reaction at high energies as summarized in Ref. [14].

Fig. 8. Comparison of the observed abundances for ${}^6\text{Li}$ and ${}^7\text{Li}$, and the calculations of Meneguzzi et al. [6] as reported by Reeves, Ref. [15]. See the text for further details.

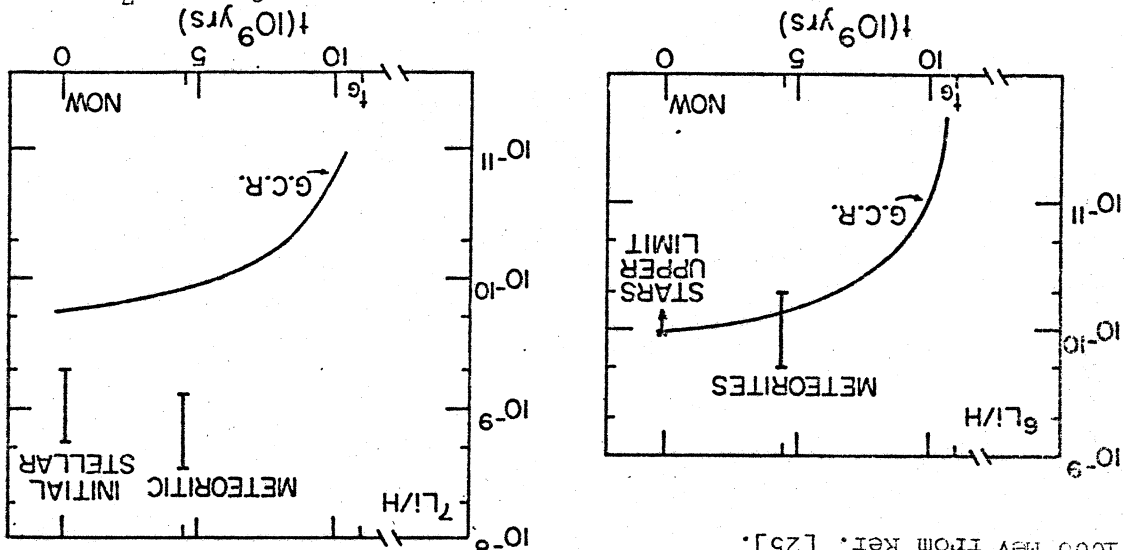
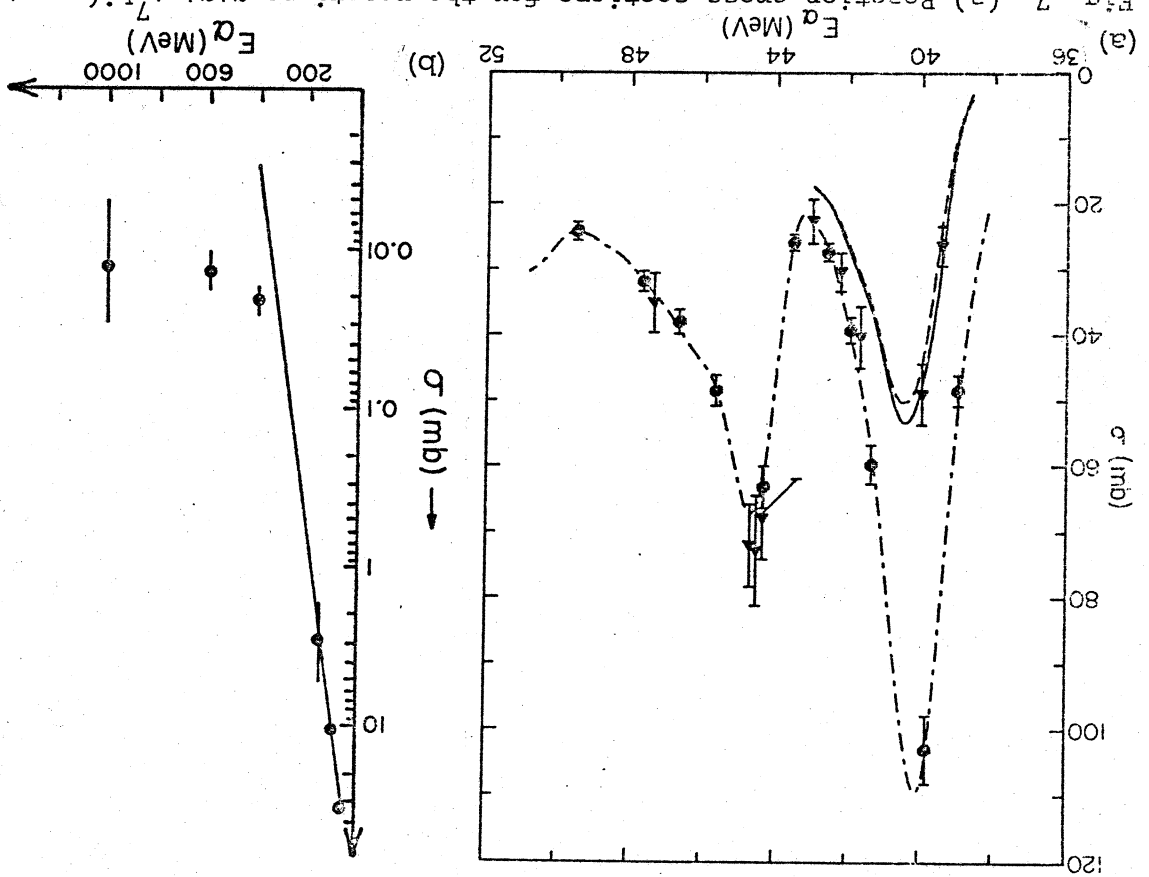


Fig. 7. (a) Reaction cross sections for the reactions $\alpha + {}^7\text{Li} \rightarrow \text{p} + {}^7\text{Li}$ (g.s. + 0.478 MeV) shown as circles and for the $\alpha + n + {}^7\text{Be}$ (g.s. + 0.429 MeV) shown as triangles. The dot-dash line is to guide the eye through the ${}^7\text{Li}$ cross sections while the solid and dashed lines describing ${}^7\text{Be}$ production near threshold are derived from the dot-dash line, using a simple compound nucleus model to estimate the ratio of ${}^7\text{Li}$ and ${}^7\text{Be}$ cross sections [23]. (b) Cross sections for ${}^7\text{Be}$ production in the $\alpha + n$ reaction at energies greater than 50 MeV. Data at 60 , 92 and 140 MeV are from Ref. [24] and the preliminary results at 400 , 600 , and 1000 MeV from Ref. [25].



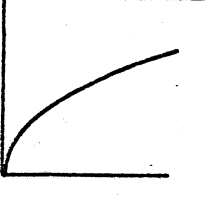
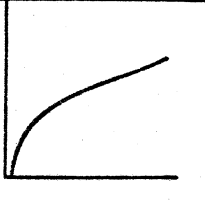
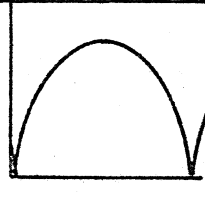
FRIEDMAN MODELS WITH $\Lambda = 0$			
	OPEN	CRITICAL	CLOSED
R(t)			
FUTURE	EXPAND FOREVER	EXPAND FOREVER	COLLAPSE
CURVATURE	HYPERBOLIC	FLAT	SPHERICAL
DENSITY	$\rho < \rho_c$	$\rho = \rho_c$	$\rho > \rho_c$

Fig. 9. Various Friedman models of the Universe as classified by the relationship between ρ and ρ_c . $R(t)$ is a scale factor of the Universe as a function of time t . Adapted from Ref. [33].

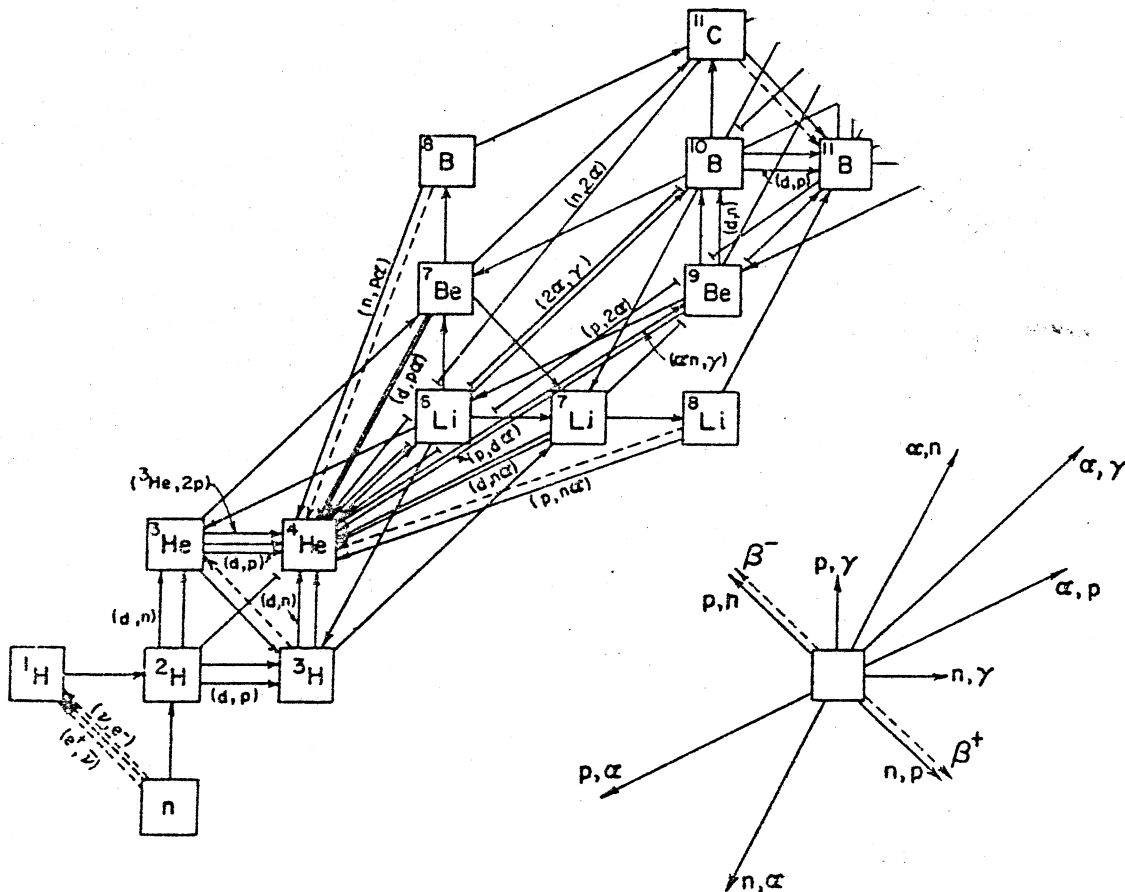
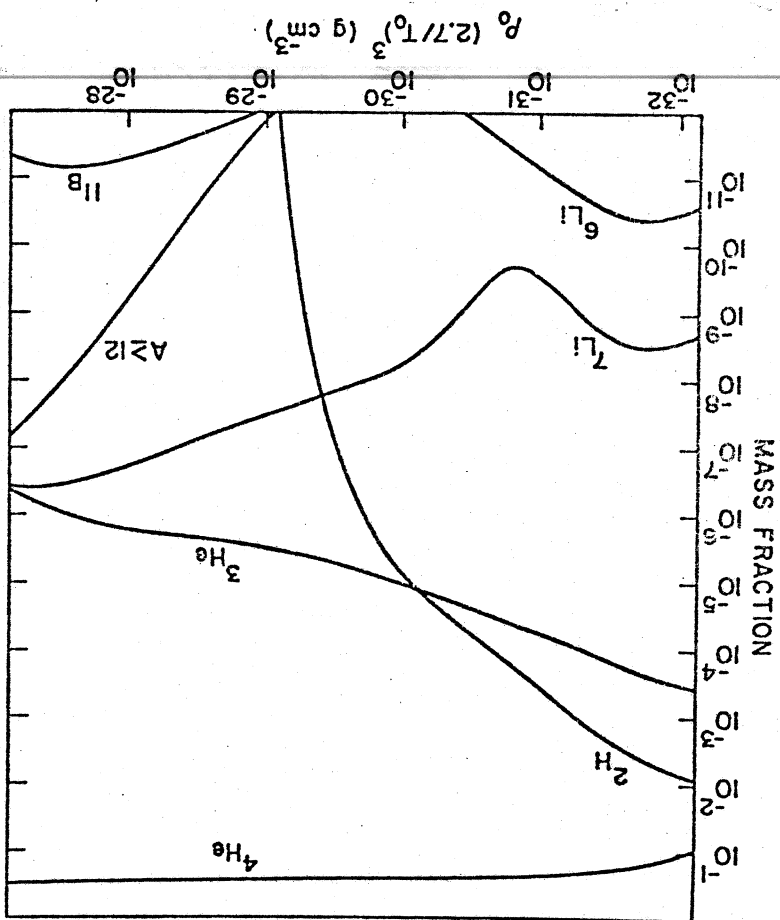


Fig. 10. Reaction network for $A < 12$. From Ref. [34].

Fig. 11. Abundances produced in a standard big bang expansion. These abundances depend only on the present value of the baryon density ρ_b . From Ref. [29].



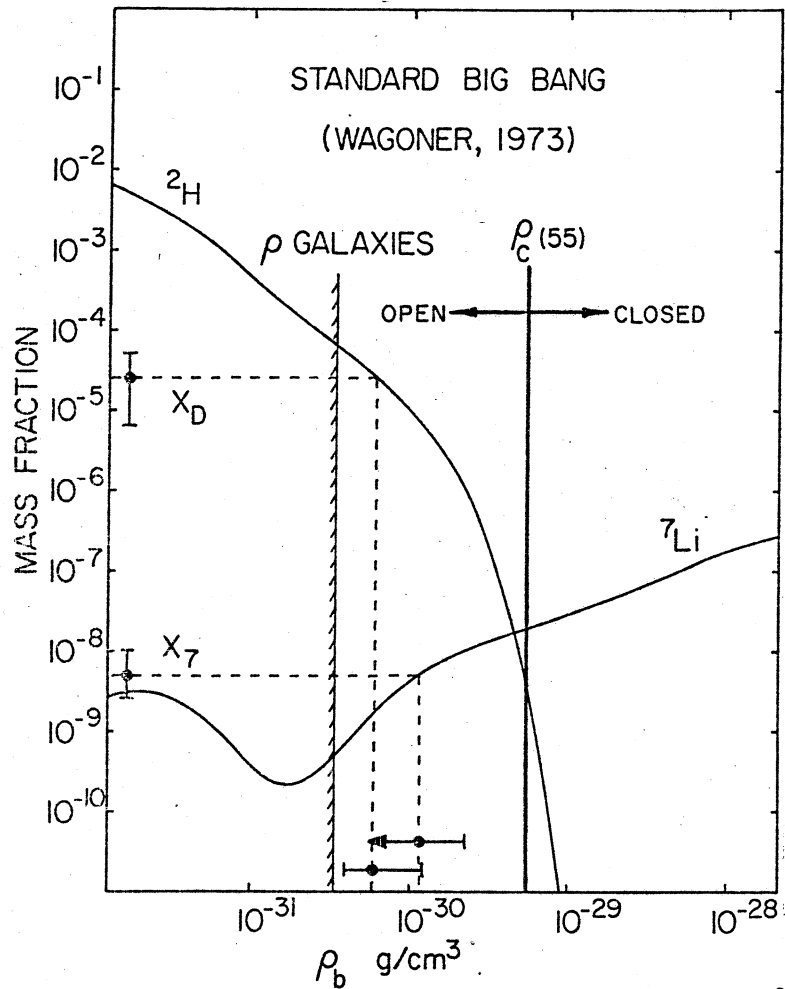


Fig. 12. Constraints on ρ_b from the abundances of ^2H and ^7Li given in Table III, and denoted by X_D and X_7 respectively. The yield predictions are from Fig. 11 [34]. Also shown are contributions to ρ_b of matter contained in galaxies ($\rho_b/\rho_c=0.06$ [33]) and the critical density ρ_c , both evaluated for $H_0=55 \text{ km sec}^{-1}\text{Mpc}^{-1}$.



1
2
3



4
5
6

